Microporous and Mesoporous Materials 138 (2011) 228–234

Contents lists available at ScienceDirect

Microporous and Mesoporous Materials

journal homepage: www.elsevier.com/locate/micromeso

Short Communication

A molecular dynamics investigation of the unusual concentration dependencies of Fick diffusivities in silica mesopores

Rajamani Krishna [a,b,*], Jasper M. van Baten [a]

[a] Van 't Hoff Institute for Molecular Sciences, University of Amsterdam, Science Park 904, 1098 XH Amsterdam, The Netherlands
[b] Department of Chemical & Biomolecular Engineering, University of California, Berkeley, CA 94720, USA

ARTICLE INFO

Article history:
Received 14 July 2010
Received in revised form 18 September 2010
Accepted 29 September 2010
Available online 29 October 2010

Keywords:
Maxwell–Stefan diffusivity
Fick diffusivity
Self diffusivity
Knudsen diffusivity
Molecular clustering

ABSTRACT

Molecular Dynamics (MD) simulations were carried out to determine the self-diffusivitiy, $D_{i,self}$, the Maxwell–Stefan diffusivity, $Đ_i$, and the Fick diffusivity, D_i, for methane (C1), ethane (C2), propane (C3), *n*-butane (nC4), *n*-pentane (nC5), *n*-hexane (nC6), *n*-heptane (nC7), and cyclohexane (cC6) in cylindrical silica mesopores for a range of pore concentrations. The MD simulations show that zero-loading diffusivity $Đ_i(0)$ is consistently lower, by up to a factor of 20, than the values anticipated by the classical Knudsen formula. The concentration dependence of the Fick diffusivity, D_i is found to be unusually complex, and displays a strong minimum in some cases; this characteristic can be traced to molecular clustering.

1. Introduction

Mesoporous materials such as SBA-16, MCM-41, and Vycor glass are used in a variety of catalysis and adsorption separation applications. In the design and development of technologies involving mesoporous materials it is essential to have a proper description of the diffusion of guest molecules. Diffusion inside mesopores is governed by a combination of molecule – molecule and molecule – pore wall interactions. For modeling *n*-component mixture diffusion inside mesopores, it is commonly accepted that the fundamentally correct approach is to relate the fluxes N_i, defined in terms of the cross-sectional area of the mesoporous material, to the chemical potential gradients $\nabla\mu_i$ by use of the Maxwell–Stefan (M–S) equations [1–6]

$$-\phi\frac{c_i}{RT}\nabla\mu_i=\sum_{j=1_{j\neq i}}^{n}\frac{x_jN_i-x_iN_j}{D_{ij}}+\frac{N_i}{D_i};\quad i=1,2,...n \tag{1}$$

where φ represents the fractional pore volume of the porous material, and the concentrations c_i are defined in terms of moles per m^3 of accessible pore volume. The x_i in Eq. (1) are the component mole fractions of the adsorbed phase within the micropores

$$x_i=c_i/c_t;\quad i=1,2,..n \tag{2}$$

The $Đ_i$ characterize species *i* – pore wall interactions in the broadest sense. The $Đ_{ij}$ are exchange coefficients representing interaction between components *i* with component *j*. For diffusion within mesopores, the $Đ_{ij}$ can be identified with the corresponding M–S diffusivity for a *fluid phase* mixture [4–6]. Conformity with the Onsager reciprocal relations prescribes.

$$Đ_{ij}=Đ_{ji} \tag{3}$$

For unary diffusion, the commonly used Fick diffusivity D_i, defined by,

$$N_i=-\phi D_i\nabla c_i \tag{4}$$

is related to the M–S diffusivity by

$$D_{ij}=Đ_i\Gamma_i \tag{5}$$

where the thermodynamic correction factor Γ_i is defined by

$$\frac{c_i}{RT}\nabla\mu_i=\Gamma_i\nabla c_i;\quad \Gamma_i\equiv\frac{\partial\ln f_i}{\partial\ln c_j}=\frac{c_i}{f_i}\frac{\partial f_i}{\partial c_i} \tag{6}$$

The Γ_i can be obtained by the adsorption isotherm that relates the pore concentrations c_i to the bulk fluid phase fugacity, f_i.

It is quite common in the published literature [1] to apply Eq. (1) to mixture diffusion in mesopores by making two assumptions: (1) $Đ_i$ can be identified with the Knudsen diffusivity, and (2) $Đ_i$ is concentration independent. Both these assumptions are debatable.In the limit of vanishingly small pore concentrations, $c_i \to 0$,

* Corresponding author at: Van 't Hoff Institute for Molecular Sciences, University of Amsterdam, Science Park 904, 1098 XH Amsterdam, The Netherlands. Tel.: +31 20 6270990; fax: +31 20 5255604.
E-mail address: r.krishna@uva.nl (R. Krishna).

1387-1811/$ - see front matter © 2010 Elsevier Inc. All rights reserved.
doi:10.1016/j.micromeso.2010.09.032

Nomenclature

b_i	dual-Langmuir-Sips constant for species *i*, $Pa^{-\nu_i}$
c_i	concentration of species *i*, mol m^{-3}
$c_{i,sat}$	saturation capacity of species *i*, mol m^{-3}
c_t	total concentration in mixture, mol m^{-3}
d_p	pore diameter, *m*
D_i	Fick diffusivity of species *i*, $m^2\ s^{-1}$
$D_{i,self}$	self-diffusivity of species *i*, $m^2\ s^{-1}$
$Đ_i$	M–S diffusivity, $m^2\ s^{-1}$
$Đ_i(0)$	zero-loading M–S diffusivity, $m^2\ s^{-1}$
$Đ_{ij}$	M–S exchange coefficients, $m^2\ s^{-1}$
$D_{i,Kn}$	Knudsen diffusivity of species i, $m^2\ s^{-1}$
f_i	fluid phase fugacity of species *i*, Pa
M_i	molar mass of species *i*, kg mol^{-1}
n	number of species, dimensionless
N_i	molar flux of species *i*, mol $m^{-2}\ s^{-1}$
R	gas constant, 8.314 J $mol^{-1}\ K^{-1}$
x_i	mole fraction of species *i* in the adsorbed phase, dimensionless
T	temperature, K
T_c	critical temperature, K

Greek letters

ϕ	fractional pore volume of material, dimensionless
Γ_i	thermodynamic factor, dimensionless
μ_i	molar chemical potential, J mol^{-1}
θ_i	fraction occupancy within pore, dimensionless
ν_i	exponent in the dual-Langmuir-Sips isotherm, dimensionless

Subscripts

i	referring to component *i*
t	referring to total mixture
Kn	referring to Knudsen
sat	referring to saturation conditions

the zero-loading diffusivity value $Đ_i(0)$ is dictated primarily by molecule-wall collisions. When the reflections are purely *diffuse* in nature, i.e., the angle of reflection bears no relation to the angle of incidence at which the molecule strikes the pore wall, the $Đ_i(0)$ value corresponds to that obtained by the classic Knudsen formula

$$D_{i,Kn} = \frac{d_p}{3}\sqrt{\frac{8RT}{\pi M_i}} \tag{7}$$

Eq. (7) holds in the limiting case when the molecule does not adsorb at pore walls [7]. Adsorption causes the molecules to "stick" to the wall, and perhaps hop to a neighboring adsorption site, rather than return to the bulk after collision [8–10]. Put another way, adsorption at the pore wall introduces a *bias* that makes a molecule hop to a neighboring site on the surface rather than return to the bulk; this bias increases with increasing adsorption strength. The bias is best appreciated by viewing animations of MD simulations, Video 1, Video 2, and Video 3, that trace the hopping trajectories, respectively, of H_2, Ar, and CH_4, follows in a 2 nm cylindrical silica pore. These Video animations have been provided as Supplementary material accompanying the on-line version of this journal. The trajectory of H_2 demonstrates that a molecule that strikes the pore wall has a tendency to return to the bulk largely in keeping with the diffuse reflection scenario prescribed by the Knudsen theory. The trajectories of CH_4 are largely restricted to the region close to the pore wall because hops to neighboring sites are dominant, and there are only occasional forays into the "core" of the pore. For Ar, the trajectory lies in between that of CH_4 and H_2; the forays into the core region are intermediate in frequency to that of CH_4 and H_2. Fig. 1 shows the radial distribution of the equilibrium concentrations of CH_4 and Ar in a 3 nm cylindrical mesopore at 300 K. We note that for the same average pore concentration, there is a higher proportion of CH_4 in the regions closer to the wall. This emphasizes the stronger bias towards hopping of CH_4 molecules to neighboring positions along the surface, rather than being reflected into the "bulk".

When the species is more strongly adsorbed the trajectory is more strongly non-linear, and on reflection the molecule's trajectory curves back towards the surface. The initial direction on leaving the surface is random, but the molecule curves back due to dispersive interaction with the surface. This behavior is discussed extensively in the papers of Bhatia and coworkers [11–14], and is termed oscillatory motion by them. The net result is a lowering in the diffusivity with increasing strength of adsorption.

Indeed, MD simulations for diffusion of a variety of guest molecules with high adsorption strength in silica pores have shown that the zero-loading diffusivity value $Đ_i(0)$ can be significantly lower than that the predictions of the Knudsen formula [4–7,12–14]. Ruthven and co-workers [15,16] have questioned the conclusions reached in these MD simulations, and have re-analysed available experimental data [3,17] to conclude that Knudsen formula remains valid for adsorbing gases. This debate on the validity of the Knudsen formula is by no means a settled matter; this is evidenced by the comments of Bhatia and Nicholson [11]. To underline this we note that in the work of Tsuru et al. [18], for example, the experimentally determined permeance of strongly adsorbing H_2O molecules across silica membranes, is significantly lower than anticipated on the basis of its molecular size. We believe that this is most likely due to the strong adsorption of H_2O molecules on the pore walls, causing violation of the Knudsen prescription.

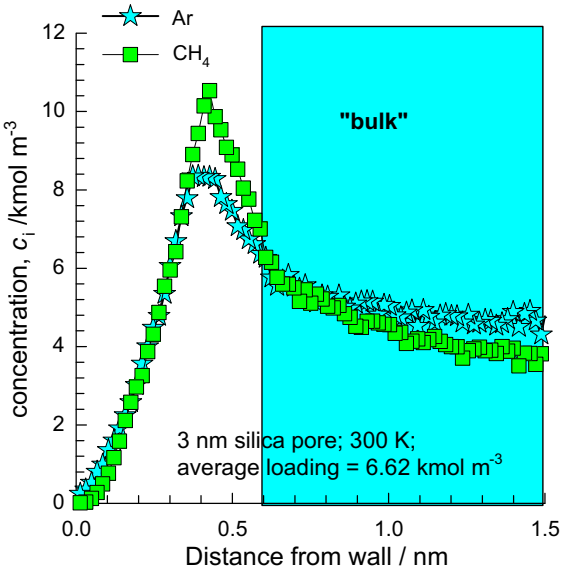

Fig. 1. Radial distribution of the equilibrium concentrations of CH_4 and Ar in a 3 nm cylindrical mesopore at 300 K. These distributions were obtained from Configurational-Bias Monte Carlo (CBMC) simulations of adsorption by sampling 10^4 equilibrated cycles.

There is a further influence of adsorption of guest molecules on mesopore diffusivities that has not received due attention in the published literature. The primary objective of the present communication is to underline the strong influence of adsorption of guest molecules on concentration dependence of the self, M–S, and Fick diffusivities. To achieve this objective, MD simulations were carried to investigate the diffusion of methane (C1), ethane (C2), propane (C3), *n*-butane (nC4), *n*-pentane (nC5), *n*-hexane (nC6), *n*-heptane (nC7), and cyclohexane (cC6) in cylindrical silica mesopores with diameters of 2, 3, 4, 5.8, 7.6 and 10 nm for a range of pore concentrations, c_i. The second objective of this study is to show that the departure of the $Đ_i(0)$ from predictions of Eq. (7) increases with increasing *C* number.

The results of this study will be important in the proper modeling of diffusion phenomena in mesoporous materials.

The MD simulation strategy used is the same as that described in our previous work [4–6]. For convenience and easy reference, the simulation methodology, specification of force fields, and simulation data on diffusivities are provided in the Supplementary material accompanying this publication.

2. Diffusivities of alkanes

Fig. 2a and b shows the MD simulations results for the self diffusivities $D_{i,self}$, and M–S diffusivities, $Đ_i$, for *n*-alkanes in a 2 nm

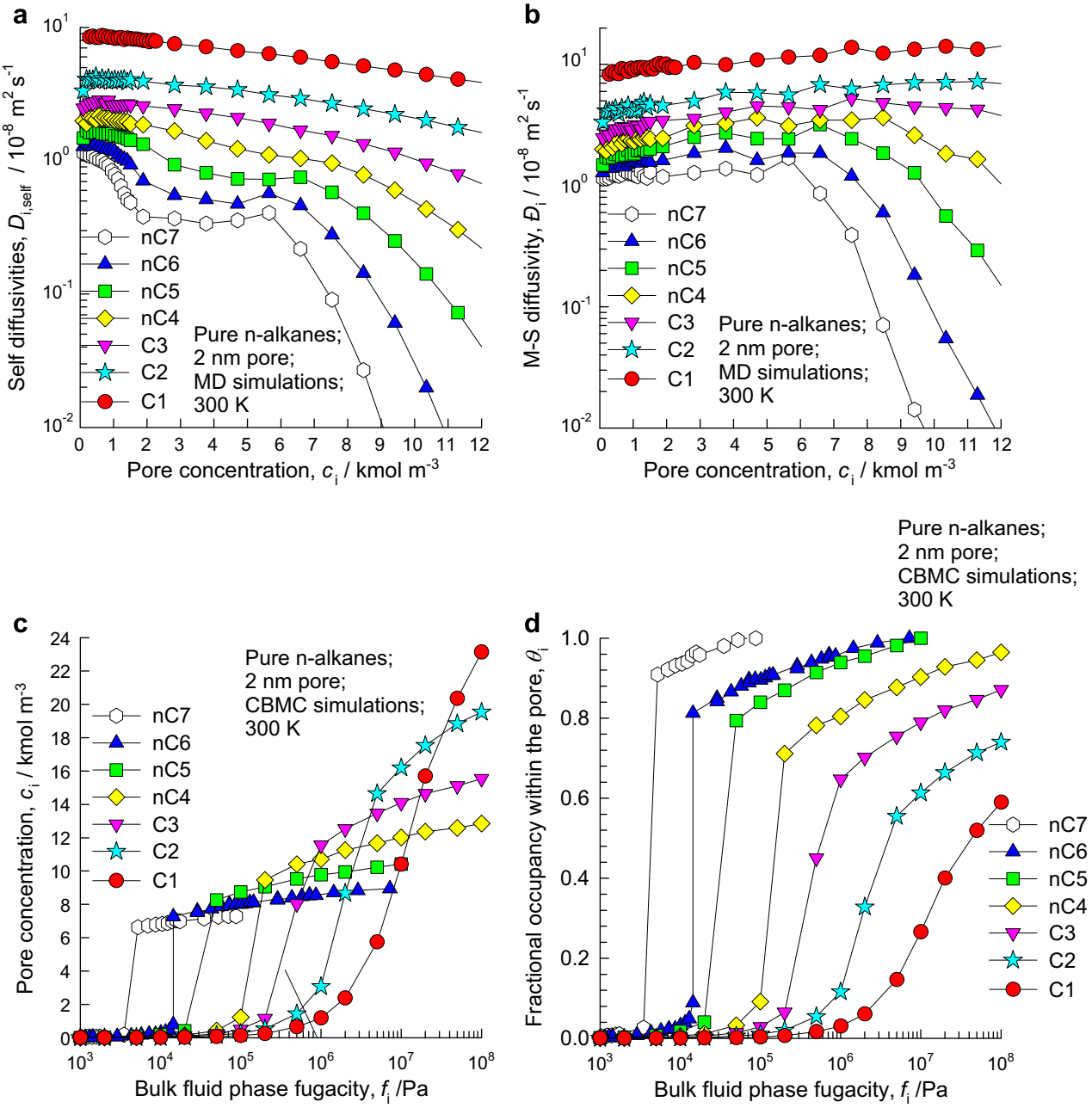

Fig. 2. MD simulations of (a) self diffusivities $D_{i,self}$, and (b) Maxwell–Stefan (M–S) diffusivities, $Đ_i$, for methane (C1), ethane (C2), propane (C3), *n*-butane (nC4), *n*-pentane (nC5), *n*-hexane (nC6), and *n*-heptane (nC7) in a 2 nm cylindrical silica pores at 300 K as a function of the concentrations c_i within the pores. (c) CBMC simulations of the pure component adsorption isotherms for *n*-alkanes in 2 nm cylindrical silica pore at 300 K. The continuous solid lines are the fits of the isotherms using the dual-Langmuir-Sips model. (d) The pure component isotherms expressed in terms of the fractional occupancy within the pores.

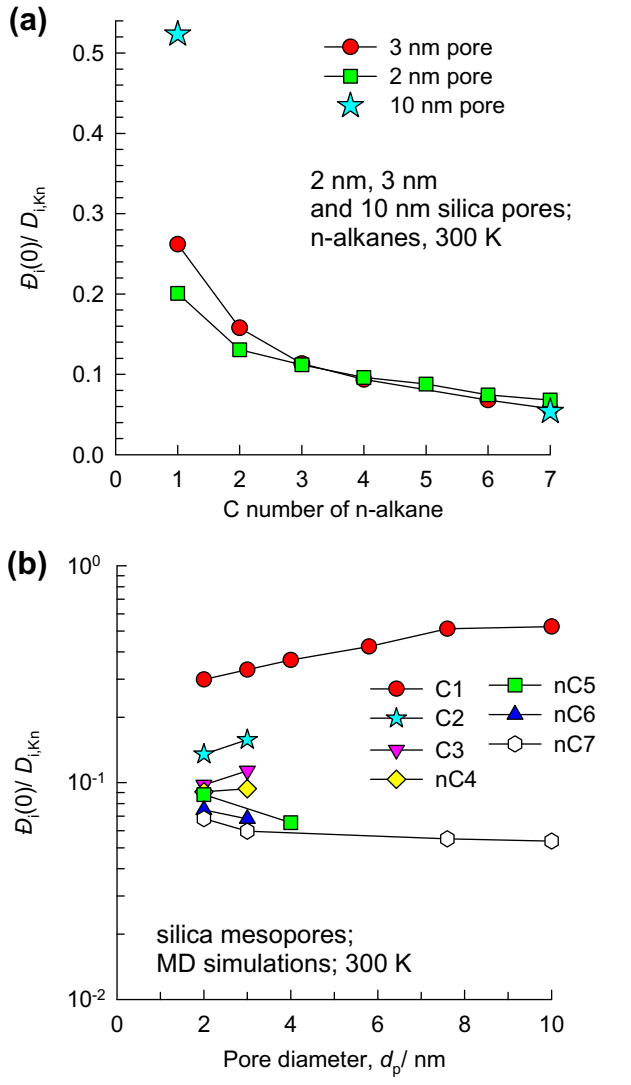

Fig. 3. (a) Ratio of the MD data on the zero-loading diffusivity to the calculated Knudsen diffusivity, $Đ_i(0)/D_{i,Kn}$, as function of the C number for 2, 3, and 10 nm silica pores. (b) $Đ_i(0)/D_{i,Kn}$ as a function of the silica pore diameter for linear alkanes. (c) Plot of MD simulated $Đ_i(0)$ versus $D_{i,Kn}$ of nC7 in 3, 7.6, and 10 nm pores at three different temperatures.

cylindrical silica pores at 300 K as a function of the concentrations c_i within the pores. In order to interpret the concentration dependences of these diffusivities, it is important to have information on the saturation capacities. For this purpose we determined the pure component adsorption isotherms using Configurational-Bias Monte Carlo (CBMC) simulations; see data in Fig. 2c for n-alkanes in 2 nm silica pores at T = 300 K. Except for CH_4 (C1, T_c = 191 K), the chosen temperature of 300 K is below the critical temperatures of the higher alkanes: ethane (C2, T_c = 305 K), propane (C3, T_c = 370 K), n-butane (nC4, T_c = 425 K), n-pentane (nC5, T_c = 470 K), n-hexane (nC6, T_c = 507.4 K), and n-heptane (nC7, T_c = 540 K). Consequently, as explained in detail in our earlier work [19,20], the isotherms become increasingly steeper with increasing alkane chain length. The saturation capacities, $c_{i,sat}$, of the n-alkanes decreases with increasing C number; these capacities are determined to be 39.1 (C1), 26.4 (C2), 17.8 (C3), 13.3 (nC4), 10.4 (nC5), 8.9 (nC6), and 7.3 (nC7) kmol m^{-3}, respectively. The fractional occupancies within the pores, θ_i, determined by dividing the actual pore concentration by the saturation concentration, are plotted in Fig. 2d. For the longer chain lengths, we note that the decrease in the self- and M–S diffusivities with increasing values of the pore concentration c_i is due to the fact that the fractional occupancies approach unity values.

The limiting values of diffusivity data of this kind extrapolated to the conditions $c_i \to 0$ are used to obtain zero-loading diffusivity values $Đ_i(0)$. Fig. 3a shows a plot of $Đ_i(0)/D_{i,Kn}$ as function of the C number for 2, 3, and 10 nm silica pores. With increasing chain length, the $Đ_i(0)$ falls increasing below $D_{i,Kn}$ due to stronger adsorption. For a given guest alkane, the $Đ_i(0)/D_{i,Kn}$ remains below unity for the entire range of pore diameters investigated, in the 2–10 nm range; see data for linear alkanes in Fig. 3b. For nC7, for example, the value of $Đ_i(0)$ is about 5% of the Knudsen prescription $D_{i,Kn}$. With increasing temperature T, the adsorption strength decreases and this makes $Đ_i(0)$ come closer to $D_{i,Kn}$ but still the value is less than 10% of $D_{i,Kn}$; see nC7 data for varying T in Fig. 3c.

The validity of the Knudsen relation, Eq. (7), is based on the requirement that the time during which the molecules are in the free space (i.e., under the influence of the uniform potential of

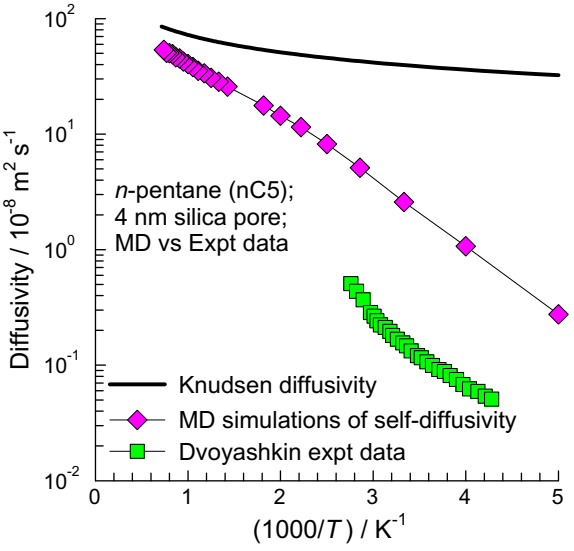

Fig. 4. Arrhenius plot for diffusivity of nC5 in a 4 nm pore. The experimental data of Dvoyashkin et al. [21] for Vycor porous glass are compared with MD simulations for 4 nm silica pore. The MD simulation data are obtained at a pore conentration c_i = 0.4 kmol m^{-3}. Also shown by the continuous solid lines are the values of the Knudsen diffusivity calculated using Eq. (7).

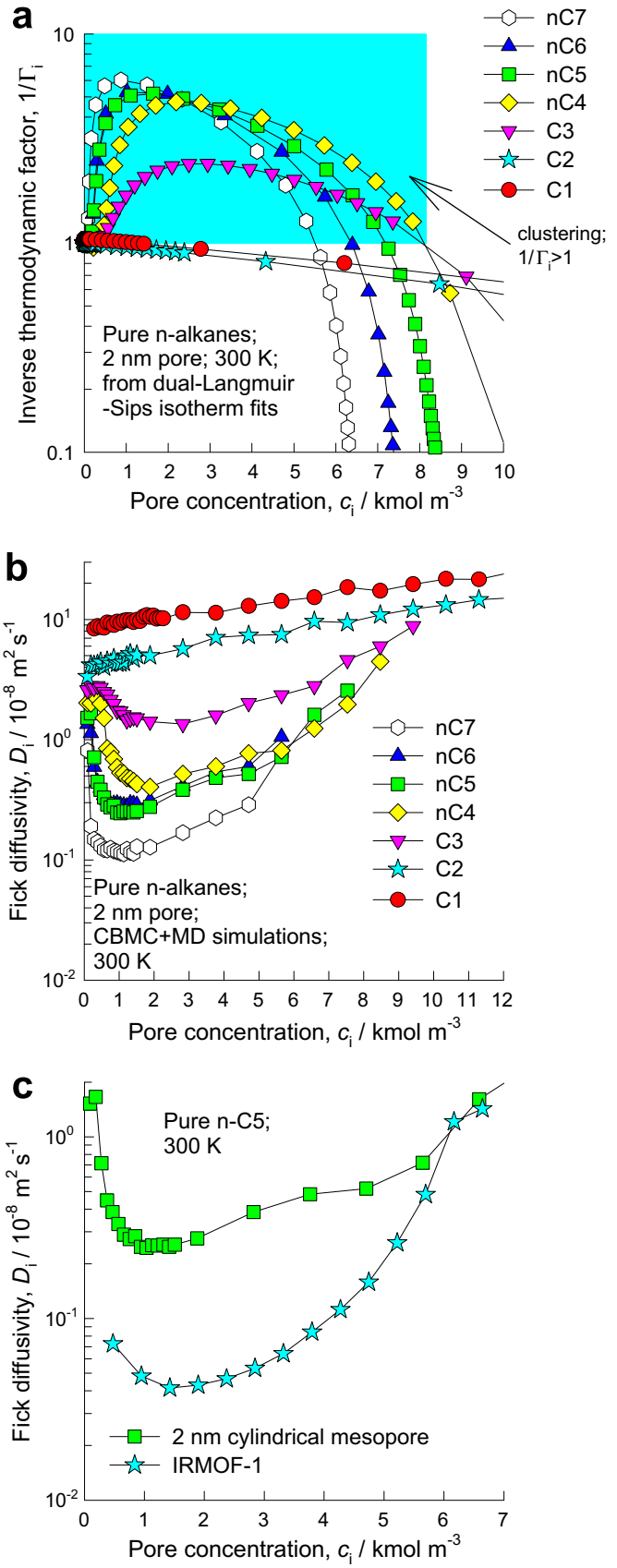

Fig. 5. (a) The inverse thermodynamic factor, $1/\Gamma_i$, plotted as a function of the pore loading, c_i, for *n*-alkanes in 2 nm silica pore. The $1/\Gamma_i$ is calculated by differentiation of dual-Langmuir-Sips fits of the isotherms shown in Fig. 2c. (b) Data on the dependence of the Fick diffusivities, D_i, on the pore concentrations c_i for *n*-alkanes in 2 nm silica pore at 300 K. (c) Comparison of the concentration dependences of the Fick diffusivities of nC5 in a 2 nm silica pore with that in IRMOF-1.

the gas phase) significantly exceeds the time during which the molecules experience the attractive forces of the surface. This is equivalent to the requirement that the number of molecules in "bulk" notably exceed the number of molecules closer to the surface. With increasing chain length a significantly larger proportion of the molecules are within the region close to the surface, and this explains the increasing break-down of the Knudsen prescription.

In order to further underline that increasing adsorption strength leads to a reduction in the $Đ_i(0)/D_{i,Kn}$ ratio, we performed MD simulations for nC5 in a 4 nm cylindrical silica pore at a variety of temperatures. The pore concentration was kept constant at a low value $c_i = 0.4$ kmol m^{-3}, ensuring that the data correspond to $Đ_i(0)$ to a good approximation. The Arrenhius plot comparing $Đ_i(0)$ and $D_{i,Kn}$ are presented in Fig. 4. With increasing T, the differences between $Đ_i(0)$ and $D_{i,Kn}$ get smaller. For example, at 300 K, $Đ_i(0)/D_{i,Kn} = 0.065$, whereas at 800 K, $Đ_i(0)/D_{i,Kn} = 0.48$. This trend is explainable because increasing temperature decreases the adsorption strength. Also plotted in Fig. 4 are NMR self-diffusivity data of Dvoyashkin et al. [21] for nC5 at different temperatures in Vycor glass having a pore size of 4 nm. The experimental data lie significantly below the MD simulations. There are three reasons for this. Firstly, the experimental data were obtained at finite pore concentrations; the fractional occupancies, θ_i, within the pores varied between 0.35 at 380 K and 1 at 220 K. We note from Fig. 2a, the $D_{i,self}$ decreases significantly with increased c_i. The second reason is that it is likely that the pores of Vycor glass are not precisely cylindrical and that tortuosity effects are in play. In any event, we note that the experimental data on $D_{i,self}$ are two to three orders of magnitude below $D_{i,Kn}$. The third reasoning is a consequence of the limitations in the sensitivity of PFG NMR diffusion studies which cannot exclusively monitor Knudsen diffusion. In such PFG NMR diffusion studies of guest molecules in porous media one generally observes molecular ensembles in which only a fraction is in the free pore space while the other fraction (by far larger one, in general) is attached to the pore surface. The measured diffusivity is the (weighted) superposition of their diffusivities and has to be smaller, therefore, than the diffusivities undergoing "pure" Knudsen diffusion, i.e., smaller than the diffusivities of the molecules in the free pore space. It is due to this reason that the PFG NMR diffusivity data taken from Ref. [21] are much smaller than the predictions from MD simulations.

When interpreting experimental data on membrane permeation of uptake within a particle, the relevant diffusivity is the Fick diffusivitiy D_i. Let us now examine how the D_i for *n*-alkanes varies with the pore concentrations c_i. For each *n*-alkane, the CBMC simulated isotherms presented in Fig. 2c were fitted using the dual-Langmuir-Sips isotherm[19,22]:

$$c_i = c_{i,A,sat}\frac{b_{i,A}f_i^{\nu_{i,A}}}{1+b_{i,A}f_i^{\nu_{i,A}}} + c_{i,B,sat}\frac{b_{i,B}f_i^{\nu_{i,B}}}{1+b_{i,B}f_i^{\nu_{i,B}}} \quad (8)$$

The steep portions of these isotherms correspond to cluster formation [19,20]. In regions where cluster formation occurs, the inverse thermodynamic factor, $1/\Gamma_i$, obtainable by analytic differentiation of Eq. (8), exceeds unity [19,20]; see Fig. 5a. The longer the alkane chain length, the larger is the value by which $1/\Gamma_i$ exceeds unity. The reason for this can be traced to the fact that for longer alkane chain lengths the T falls increasingly below T_c and this leads to a higher degree of clustering [19,20]. As the fractional occupancy $\theta_i \to 1, (1/\Gamma_i) \to 0$.

The Fick diffusivities can be obtained from the combining the data presented in Figs. 2b and 5a; the resulting D_i versus c_i data are shown in Fig. 5b. The strong influence of the pore concentration on the D_i is evident. Particularly noteworthy is the strong decrease in the D_i for higher alkanes in the low concentration range. This decrease is entirely to be ascribed to cluster formation. Animations

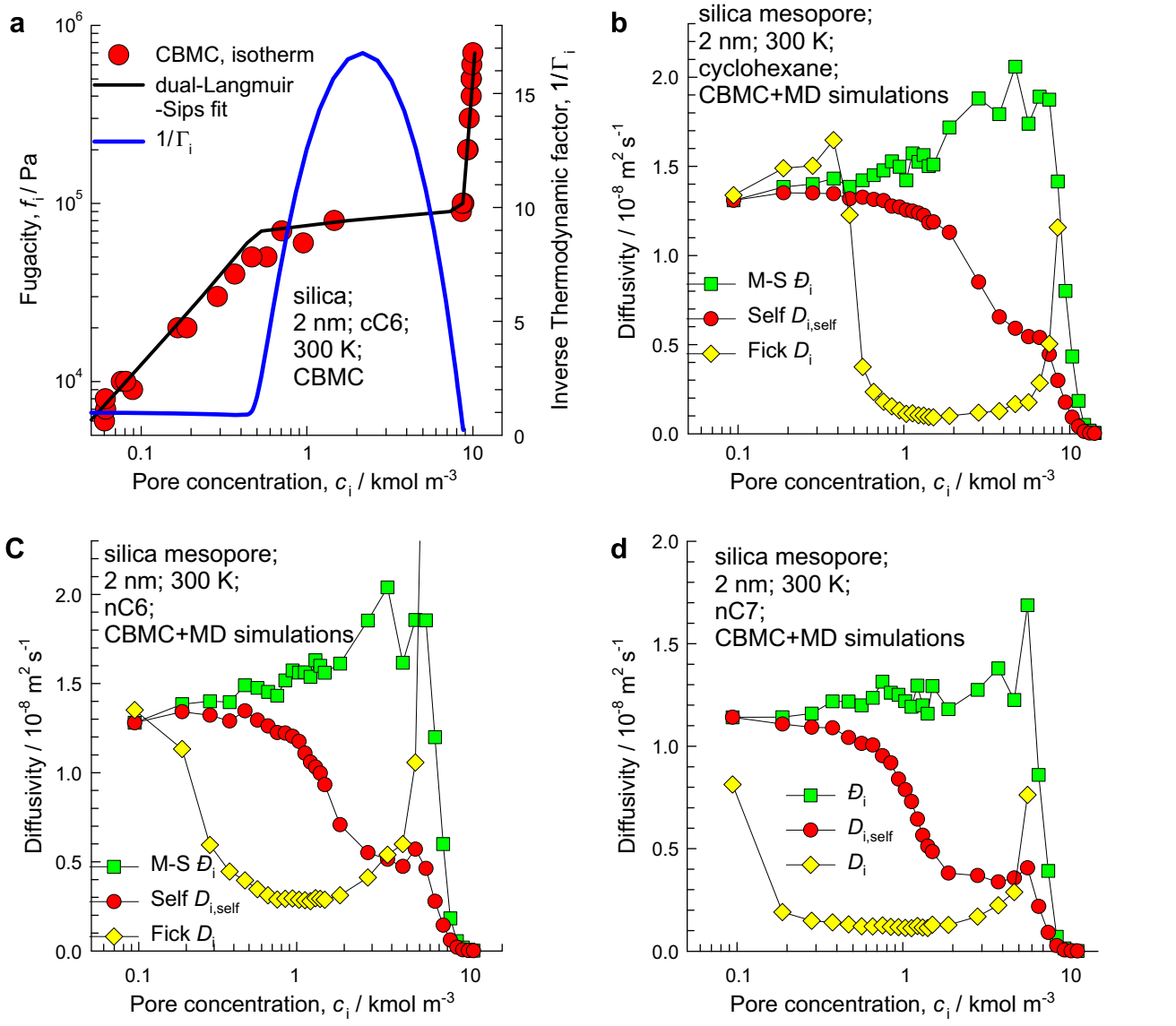

Fig. 6. (a) CBMC simulations of the pure component adsorption isotherms for cyclohexane in 2 nm cylindrical silica pore at 300 K, along with the inverse thermodynamic factor, $1/\Gamma_i$, determined by analytic differentiation of dual-Langmuir-Sips isotherm fit. (b) Data on the dependence of the self, M–S, and Fick diffusivities on the pore concentrations c_i for cyclohexane (cC6) in 2 nm silica pore at 300 K. (c) Data on the dependence of the self, M–S, and Fick diffusivities on the pore concentrations c_i for *n*-hexane (nC6) in 2 nm silica pore at 300 K. (d) Data on the dependence of the self, M–S, and Fick diffusivities on the pore concentrations c_i for *n*-heptane (nC7) in 2 nm silica pore at 300 K.

obtained from MD simulations, available in the on-line version of this journal as videos 4–13, provide a visual appreciation of cluster formation occurring for longer alkane chain lengths.

Results analogous to those presented in Fig. 5b were obtained in our earlier work on diffusion inside *microporous* metal–organic frameworks, such as IRMOF-1 and PCN-6′ [20]. As illustration, Fig. 5c provides a comparison of the concentration dependences of the Fick diffusivities of nC5 in a 2 nm silica pore with that in IRMOF-1, that consists of two alternating, inter-connected, cavities of 1.1 and 1.43 nm diameter separated by 0.8 nm sized windows. We note that the Fick D_i exhibits a much shaper decline with increasing concentration in the 2 nm silica pore than that observed in the *micro*porous IRMOF-1. The comparative trends shown in Fig. 5c for nC5 is generally valid for any alkane; the concentration decrease of the Fick diffusivities in mesopores is much stronger. The infra-red microscopy data of Chmelik et al. [22] for alkanes diffusion in CuBTC and the QENS data of Salles et al. [23] for diffusion of CO_2 in MIL-47 provide verification of the trends observed in Fig. 5b and c. These experimental works provide a verification of the strong minimum in the variation of the Fick diffusivity with pore concentration. This strong minimum is a direct consequence of the maximum in the inverse thermodynamic factor, and is a consequence of molecular clustering.

In our previous study on diffusion in microporous metal organic frameworks, we had demonstrated that even differences in the critical temperature of 10–20 K between linear and branched alkanes of the same C number causes significant differences in the degree of clustering. In view of the fact that the critical temperature of cC6 is 553 K we should expect the degree of clustering of cC6 to be higher than any of the *n*-alkanes considered above. To verify this expectation, we investigated the diffusion of cyclohexane (cC6) in a 2 nm silica pore at 300 K. The strong clustering tendencies of cC6 is most clearly evident in videos 14, and 15. In quantitative terms, the high degree of clustering of cC6 manifests

in values of $1/\Gamma_i$ that exceed unity more than for nC7; see Fig. 6a. The consequences of $1/\Gamma_i \gg 1$ for the concentration dependence of the diffusivities are apparent on examination of the diffusivity data for cC6 in Fig. 6b. In regions where $1/\Gamma_i \gg 1$, the Fick D_i shows a minimum. Results analogous to those presented in Fig. 6b are obtained for nC6 and nC7; see Fig. 6c, and d. The sharpest decline in the Fick diffusivity is for cC6 that has the highest T_c, and the strongest degree of clustering.

In the low concentration range 0–0.4 kmol m^{-3}, we note that all three diffusivities for cC6 show slight, yet discernible, increase with c_i. The NMR data of Valiullin et al. [24] for cC6 diffusion in Vycor porous glass provides some indication that the concentration dependences of the diffusivities shown in Fig. 6b are indeed the right trends in the regions of low concentration.

3. Conclusions

Molecular Dynamics simulations have been used to investigate the characteristics of diffusion of a variety of alkanes in silica mesopores. The following major conclusions can be drawn from this study.

(1) With increasing C number of alkanes, the zero-loading diffusivity $Đ_i(0)$ falls increasingly below that predicted by the Knudsen formula, Eq. (7). The validity of the Eq. (7) is restricted to cases where the adsorption strength of the molecule is sufficiently small and to cases where the molecular trajectories on reflection from the surface are linear. Strong adsorption makes these trajectories curve back towards adjoining surface regions and lowers the diffusivity through the pore.
(2) Increasing temperature, lowers the adsorption strength; this has the effect of increasing the ratio $Đ_i(0)/D_{i,Kn}$ but the values still remain below unity for all cases examined.
(3) The dependence of the Fick diffusivity, D_i, on the pore concentration c_i is significantly influenced by the inverse thermodynamic factor $1/\Gamma_i$. For concentration regions where $1/\Gamma_i$ exceeds unity there is evidence of significant clustering of molecules. Also, when $1/\Gamma_i \gg 1$, the Fick diffusivity can exhibit a strong minimum. Put another way, the minimum in the D_i–c_i data can be traced to the corresponding maximum in the $1/\Gamma_i$–c_i data, and both behaviors are traceable to molecular clustering.

The results of our study underline the dangers in using Eq. (1) together with the assumption that D_i equals $D_{i,Kn}$, and that this parameter is concentration independent.

Acknowledgements

This material is based upon work supported as part of the Center for Gas Separations Relevant to Clean Energy Technologies, an Energy Frontier Research Center funded by the US Department of Energy, Office of Science, Office of Basic Energy Sciences under Award Number DE-SC0001015.

Appendix A. Supplementary data

Supplementary data associated with this article can be found, in the online version, at doi:10.1016/j.micromeso.2010.09.032.

References

[1] E.A. Mason, A.P. Malinauskas, Gas Transport in Porous Media: The Dusty-Gas Model, Elsevier, Amsterdam, 1983.
[2] F. Keil, Diffusion und Chemische Reaktion, Springer Verlag, Heidelberg, 1999.
[3] S. Higgins, W. DeSisto, D.M. Ruthven, Microporous Mesoporous Mater. 117 (2009) 268–277.
[4] R. Krishna, J.M. van Baten, Chem. Eng. Sci. 64 (2009) 870–882.
[5] R. Krishna, J.M. van Baten, Chem. Eng. Sci. 64 (2009) 3159–3178.
[6] R. Krishna, J. Phys, Chem. C 113 (2009) 19756–19781.
[7] S. Jakobtorweihen, C.P. Lowe, F.J. Keil, B. Smit, J. Chem. Phys. 127 (2007) 024904.
[8] Y. Shindo, T. Hakuta, H. Yoshitome, H. Inoue, J. Chem. Eng. Japan. 16 (1983) 120–126.
[9] G.K. Papadopoulos, D. Nicholson, S.H. Suh, Mol. Simulation 22 (1999) 237–256.
[10] J.S. Bae, D.D. Do, J. Non-Equilib. Thermodyn. 30 (2005) 1–20.
[11] S.K. Bhatia, D. Nicholson, Chem. Eng. Sci. 65 (2010) 4519–4520.
[12] S.K. Bhatia, O. Jepps, D. Nicholson, J. Chem. Phys. 120 (2004) 4472–4485.
[13] S.K. Bhatia, D. Nicholson, A.I.Ch.E.J. 52 (2006) 29–38.
[14] S.K. Bhatia, Langmuir 26 (2010) 8373–8385.
[15] D.M. Ruthven, W. DeSisto, S. Higgins, Chem. Eng. Sci. 64 (2009) 3201–3203.
[16] D.M. Ruthven, W. DeSisto, S. Higgins, Chem. Eng. Sci. 65 (2010) 4521–4522.
[17] S.C. Reyes, J.H. Sinfelt, G.J. DeMartin, R.H. Ernst, E. Iglesia, J. Phys, Chem. B 101 (1997) 614–622.
[18] T. Tsuru, R. Igi, M. Kanezashi, T. Yoshioka, S. Fujisaki, Y. Iwamoto, A.I.Ch.E.J. XX (2010) XXX-XXX. (http://dx.doi.org/10.1002/aic.12298).
[19] R. Krishna, J.M. van Baten, Langmuir 26 (2010) 3981–3992.
[20] R. Krishna, J.M. van Baten, Langmuir 26 (2010) 8450–8463.
[21] M. Dvoyashkin, R. Valiullin, J. Kärger, Phys. Rev. E 75 (2007) 041202.
[22] C. Chmelik, J. Kärger, M. Wiebcke, J. Caro, J.M. Van Baten, R. Krishna, Microporous Mesoporous Mater. 117 (2009) 22–32.
[23] F. Salles, H. Jobic, T. Devic, P.L. Llewellyn, C. Serre, G. Férey, G. Maurin, ACS Nano 4 (2010) 143–152.
[24] R. Valiullin, S. Naumov, P. Galvosas, J. Kärger, H.J. Woo, F. Porcheron, P.A. Monson, Nature 443 (2006) 965–968.